The Nucleus **51**, No. 3 (2014) 311-317

www.thenucleuspak.org.pk

**The Nucleus**

**ISSN 0029-5698 (Print)**
**ISSN 2306-6539 (Online)**

# Production of Bulk Amorphous Steels and Their Characterization

M. Iqbal[1*] and W.H. Wang[2]

[1]Microstructural Studies Group, Physics Division, Directorate of Science, PINSTECH, P.O. Nilore, Islamabad, Pakistan

[2]Institute of Physics, Chinese Academy of Sciences, Beijing, China

*(Received June 10, 2014 and accepted in revised form August 25, 2014)*

Paramagnetic bulk amorphous steels (BASs) having the compositions $Fe_{50}Cr_{14}Mo_{14}C_{14}B_6M_2$ (M = Zr, Nb and Pt) were produced. We have replaced Y, Gd and Dy with Zr, Nb and Pt in the BASs. Materials were characterized by SEM, EDS, DSC and XRD techniques. Density of the as cast $Fe_{50}Cr_{14}Mo_{14}C_{14}B_6Zr_2$ was found to be 7.17 g/cm$^3$ which is less than all previously reported BASs. Vicker's microhardness, nanohardness, elastic modulus and fracture stress are found to be 1240 $H_V$, 14.9 GPa, 248 GPa and 4.96 GPa respectively. Examination of Vicker's indents show semicircular shear bands around the indents indicating presence of a little ductility in the $Fe_{50}Cr_{14}Mo_{14}C_{14}B_6Zr_2$ BAS. This BAS have very promising thermal properties. Melting and liquid temperatures are found to be 1392 and 1543 K respectively which are too high for BASs. Width of supercooled liquid region of 70 K and value of $\gamma$ parameter approximately 0.4 indicates very promising thermal stability and high glass-forming ability (GFA). SEM examination of the broken pieces of the compression tests fractured specimens shows parallel and curved shear bands indicating brittleness in the bulk samples. DSC results confirm multistage crystallization. Present investigations on $Fe_{50}Cr_{14}Mo_{14}C_{14}B_6Zr_2$ showed that this BAS had better mechanical and thermal properties than many other structural steels.

**Keywords:** Bulk metallic glasses, Amorphous steels, Thermal properties, Mechanical properties, Bulk amorphous alloys

## 1. Introduction

Bulk amorphous steels (BASs) are new class of amorphous materials having paramagnetic behavior and high melting and liquid temperatures. High carbon content (up to 15 %) is used in BASs [1-3]. Paramagnetic BASs have good physical, mechanical and thermal properties. Like other bulk metallic glasses (BMGs), BASs are used for various applications. There are many reports available on synthesis and characterization of BASs [1-10]. Although as cast BASs have very high Vicker's hardness (over 1100 $H_V$) but most of them are found to be brittle. Many researchers used minor alloying method and added various solute elements such as Y, Dy, Gd and Er to get the desired properties [11-16]. But still there are many limitations in the commercial applications of bulk metallic glasses (BMGs). So, further investigations are still needed. The major problem of BMGs is their low ductility. Although a lot of research work has been done on BASs but there is no report available on synthesis and characterization of $Fe_{50}Cr_{14}Mo_{14}C_{14}B_6M_2$ (where M = Zr and Pt) BASs. We have reported mechanical and thermal properties of some BASs such as $Fe_{50}Cr_{14}Mo_{14}C_{14}B_6X_2$ (where X = Y, Gd and Dy) which were produced at China [1-3]. The maximum value of the SLR, $\Delta T_x$ (the difference between the crystallization and glass transition temperatures $T_x$-$T_g$) reported is about 60 ± 5 K which needs further improvement. It is desired to improve the glass-forming ability (GFA) of the BMGs especially BASs which will be useful for commercial and industrial applications. Recently a few more BASs $Fe_{50}Cr_{14}Mo_{14}C_{14}B_6M_2$ (where M = Zr, Nb and Pt) are produced such as scanning electron microscopy, energy dispersive x-ray analysis (EDAX), x-ray diffraction (XRD) and differential scanning calorimetery (DSC) were used to characterize the materials.

## 2. Experimental

Alloy buttons having the $Fe_{50}Cr_{14}Mo_{14}C_{14}B_6M_2$ (where M = Zr, Nb and Pt) bulk amorphous steels (BASs) were produced by melting the pure elements in an arc melting furnace (WK-II, China) under vacuum down to $1x10^{-4}$ Pa. Fe-B master alloy and 3-4 N pure metals were used to prepare the alloy ingots of about 90 mm length and 3 mm thickness. Melting of the alloy buttons was done at least four times to get the extended chemical homogeneity. Melting was done in Ti gettered inert atmosphere by using pure argon of 5N purity to achieve the homogenous materials. Casting was conducted by achieving cooling rate at least in the range of $10^{-3}$-$10^{-5}$ °C/s. Argon gas was flushed before melting and casting. Cylindrical rods were produced by Cu mold casting technique. Suction casting method was used for casting. Samples of appropriate sizes were cut down by diamond cutter and polished on lapping machine. As cast samples were examined in scanning electron microscope (SEM, LEO 440i) and analyzed by energy

* Corresponding author: miqbalchishti@gmail.com

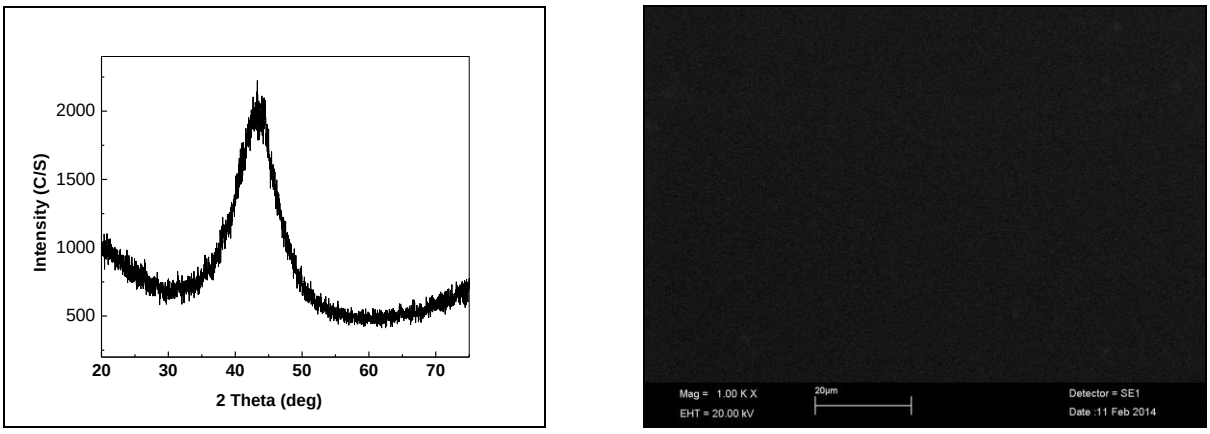


(a) (b)

Figure 1. XRD of the cast bulk sample of 3 mm thickness (a) SEM image of the as cast sample showing featureless surface (b).

dispersive spectroscopy (EDS), by using Oxford Link ISIS 300 system, attached with the SEM. Structural analysis was done by XRD by using RIGAKU Diffractometer Cu $K_{\alpha 1}$ (having wave length $\lambda$ = 1.54056 Å) radiations. In order to study the thermal behavior, differential scanning calorimetry (DSC) was conducted employing Perkin Elmer 7/Pyris DSC and NETZSCH DSC 404 F3 systems. Exothermic and endothermic reactions were observed and various thermal parameters were calculated. Density ($\rho$) was measured applying "Archimedes principle" by using distilled water at room temperature. Experiments on density measurement were repeated several times. Vicker's microhardness ($H_V$) was measured by "Everone hardness tester" under an appropriate load of 200-300 gram force (gmf). In order to conduct fracture analysis, compression tests were applied for as cast fully amorphous cylindrical sample with aspect ratio approximately 2 (length/diameter). The specimens were polished to smooth the ends using a special holder specially designed for this purpose for flattening of the samples. All compression tests (using uniaxial compressive quasistatic loading) were carried out at room temperature at a strain rate of $4.2x10^{-4}$/s. In this manuscript, we are reporting first time the results on "Production and characterization of first $Fe_{50}Cr_{14}Mo_{14}C_{14}B_6Zr_2$ BAS" produced at MSG, PD, PINSTECH, Pakistan and IOP, CAS, Beijing, China.

## 3. Results and Discussion

As cast ingots of the BASs were observed physically as well as in stereo scan microscope and found to be very bright and shine having the excellent metallic luster. It is one of the unique properties of BMGs [17]. BASs also exhibit this property. Therefore, like other BMGs, BASs can be used for structural and jewelry applications. Usually BASs are very hard due to high carbon content, so their cutting and engineering is quite difficult. Therefore, jewelry parts and other pieces of products would be cast directly into oxygen free special Cu molds having the shape and design of the required product. It is well established that BMGs have the excellent corrosion resistance at room temperature and pressure. XRD pattern of the as cast samples selected from the center of the one of the alloy ingot is shown in Figure 1(a). The broad band in the XRD patterns without any appreciable diffraction peaks indicates the amorphous nature of the material produced. XRD was repeated for powder sample by grinding the bulk pieces of ingots under similar experimental conditions at room temperature. Similar broad band was observed in the XRD pattern confirming the amorphous nature of material synthesized. Ingots of thickness greater than 3 mm were found to be partially crystalline. Some sharp diffraction peaks as well as broad humps were observed in the XRD patterns taken for the samples having thickness over 3 mm. The reason is the nucleation of the crystalline phases and precipitates (PPTs) during casting. Although fast quenching was achieved by using Cu mold casting technique even then crystallization occurred in bulk ingots of thickness over 3 mm. In addition, cooling of Cu molds was conducted by using running water through water chiller. Atomic radii [18] and heats of mixings [19] of all the alloy constituents are given in Table 1.

The crystallization took place due to high chemical reactivity between Zr and C atoms to produced PPTs of zirconium carbides. There is possibility of the nucleation of precipitates of $M_{23}C_6$ and $M_6C$ nature in case of slow cooling. We have already reported the formation of $\gamma$-Fe, $Cr_{23}C_6$ and $\eta$-$Fe_3Mo_3C$ phases in our previously reported $Fe_{50}Cr_{14}Mo_{14}C_{14}B_6M_2$ (M = Y, Gd and Dy) BASs identified by XRD and Mössbauer spectroscopy [1-3]. Atomic radius of Zr atoms is larger than any other solute elements. For microstructural

Table 1. Heat of mixings ($\Delta H_{mix}$) and atomic radii ($R_a$) of alloy constituents.

| Element | Atomic radii $R_a$ (nm) | Density ($\rho$) g/cm$^3$ | Mixing enthalpies (kJmol$^{-1}$) | | | | |
|---|---|---|---|---|---|---|---|
| | | | Fe | Cr | Mo | C | B |
| | | | 0.12412 | 0.12490 | 0.13626 | 0.07730 | 0.08200 |
| Fe | 0.12412 | 7.874 | - | -1 | -2 | -61 | -26 |
| Cr | 0.12490 | 7.190 | -1 | - | 0 | -61 | -31 |
| Mo | 0.13626 | 10.28 | -2 | 0 | - | -67 | -34 |
| C | 0.07730 | 3.514 | -61 | -61 | -67 | - | 0 |
| B | 0.08200 | 2.350 | -26 | - | -34 | 0 | - |
| Zr | 0.16025 | 6.508 | -25 | -12 | -6 | -131 | -71 |
| Gd | 0.18013 | 7.859 | -1 | 11 | 24 | -117 | -50 |
| Dy | 0.17740 | 8.559 | -3 | 9 | 22 | -117 | -51 |

Table 2. Thermal parameters of the alloy deduced from DSC scan conducted at 10 K/min.

| $T_g$ | $T_x$ | $\Delta T_x$ | $T_{p1}$ | $T_{p2}$ | $T_{p3}$ | $T_m$ | $T_l$ | $T_{rg1}$ | $T_{rg2}$ | $\gamma$ |
|---|---|---|---|---|---|---|---|---|---|---|
| 798 | 868 | 70 | 885 | 933 | 993 | 1392 | 1453 | 0.57 | 0.55 | 0.39 |
| $\beta$ | $\delta$ | $\omega$ | $K_H$ | $K_W$ | $K_{LL}$ | $K_{SP}$ | $K_1$ | $K_2$ | $K_3$ | $K_4$ |
| 2.02 | 1.33 | 0.21 | 0.134 | 0.05 | 0.396 | 1.49 | 594 | 70 | 0.624 | 0.855 |

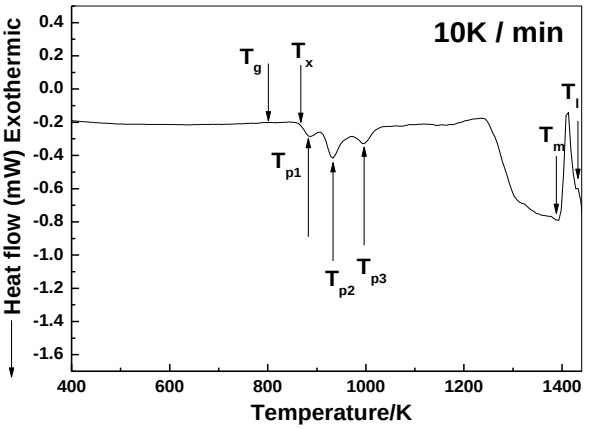


Figure 2. High temperatures DSC of the alloy conducted at heating rate of 10 K/min.

investigations, as cast fine polished samples were examined in SEM. No defects such as pores, voids, second phase particles or precipitates (PPTs) were observed in the bulk samples. For verification, selected pieces were examined in SEM and no defects were observed. Figure 1(b) shows SEI (secondary electron image) taken by SEM, showing featureless surface without any defects. It reconfirms the amorphous nature of the material produced. SEM and EDAX results confirm each other. EDAX analysis confirms the designed composition within the experimental error. Density ($\rho$) is one of the important properties especially from industrial point of view. It reflects the packing state of the constituent elements. The density was measured and found to be 7.17 ± 0.03 g/cm$^3$ which is less than steels containing Gd and Dy [1, 2]. The lower density of the present BAS is due to lower density and smaller atomic size of Zr than Gd and Dy atoms as given in Table 1. High temperature DSC scan of the alloy conducted at a heating rate of 10 K/min is shown in Figure 2. Exothermic and endothermic reactions are very prominent. DSC scan shows the presence of multistage crystallization in the alloy. A number of thermal parameters are evaluated and are given in Table 2. Thermal parameters like glass transition temperature $T_g$, crystallization temperature $T_x$, supercooled liquid region $\Delta T_x$ (= $T_x$-$T_g$), peak temperatures $T_p$, melting temperature $T_m$, liquidus temperature $T_l$ , a key parameter known as "reduced glass transition temperature" $T_{rg1} = T_g/T_m$ and $T_{rg2} = T_g/T_l$, $\gamma = T_x/(T_l+T_g)$ [20], $\delta = T_x/(T_l-T_g)$ [21], $\beta = T_g{}^*T_x/(T_l-T_x)^2$ [22] and a newly defined thermal parameter $\omega = T_g/T_x - 2T_g/(T_g+T_l)$ [23] are deduced and the results are presented in Table 2. In addition some more thermal parameters such as Hruby parameter $K_H = \Delta T_x/(T_m-T_x)$ [24], Thermal parameter proposed by Saad and Poulain $K_{SP} = (T_p-T_x)(\Delta T_x)/T_g)$ [25], Weinberg parameter $K_W = \Delta T_x/T_m$, thermal parameter $K_{LL} = T_x/(T_g+T_m)$ [26], $K_1 = T_m-T_g$, $K_2 = \Delta T_x$, $K_3 = T_x/T_m$ and $K_4 = (T_p-T_x)(\Delta T_x)/T_m)$ [27] are also calculated and are given in Table 2.

It may be note that $T_g$, $T_x$, $T_p$, $T_m$ and $T_l$ are very high which are the characteristics of the amorphous

steels like other Fe-based BMGs. The width of SLR, the difference between crystallization and glass transition temperature ($\Delta T_x = T_x - T_g = 70$ K) is larger than any BASs produced. The question arises, "Why SLR ($\Delta T_x$) and other thermal parameters of the present BAS is better than other steels?" The reason is the replacement of Zr with Y, Gd and Dy which enhanced disorder in the amorphous structure. A number of thermal parameters are compared in Table 3. The study shows that the present BAS have the highest thermal stability as compared to previously reported BASs [1-3]. Thermal parameters given in Table 2 show the complete thermal behavior of the material produced. It may be noted that base Fe-Cr-Mo-C-B alloy with varied amount of Cr and Fe have the SLR in the range of 45-53 K [28, 29]. Addition of Zr atoms caused to extend SLR ($\Delta T_x$) to 70 K. It is due to enhancement in the disordered structure that produced by addition of Zr atoms having the highest atomic radius (0.16025 nm) than all other alloy constituents of present BAS.

Hardness, elastic modulus and fracture strength are essential parameters of structural and engineering materials including BMGs. The average experimental value of Vicker's hardness "$H_V$" of present BAS was measured to be 1240 ± 20 $H_V$ which is higher than any other system such as Zr-based [30, 31], Ni-based [32] and Mg-based [33] amorphous alloys but comparable with other BASs [1,2]. Vicker's hardness is correlated with elastic modulus "E" as well as fracture stress "$\sigma_f$" as ($E/Hv \approx 20$ and $E/\sigma_f \approx 50$ and $H_V = 2.5\sigma_f$) [34]. There is an empirical relationship exists between nanohardness H and fracture strength $\sigma_f$ (i.e., $H/\sigma_f \approx 3$) [35]. By using these well-known relations, the values of elastic modulus E, nanohardness "H", fracture stress "$\sigma_f$", are calculated and compared with other steels as given in Table 4. It is clear that values of $H_V$, H, E and $\sigma_f$ are found to be 1240 $H_V$, 14.9 GPa, 248 GPa and 4.96 GPa respectively. Comparison shows that these values are very high or comparable with other steels. It may be noted that nanohardness to elastic modulus (H/E), fracture strength to elastic modulus ($\sigma_f/E$) and nanohardness to fracture strength ($H/\sigma_f$) ratios of present BAS are found to be 0.06, 0.02 and 3.0 respectively which are comparable with other steels [1,2]. The value of $\sigma_f/E$ ratio was found to be 0.02 which is much higher than $\sigma_f/E$ ratio for crystalline alloys (~0.008). It is important to note that a covalently bonded materials exhibit a higher H/E than that of a metal. The H/E ratio is about 0.1 for most covalently bonded materials as compared to about 0.002 for face centered cubic metals. The H/E ratio for present BAS is close to 0.1 suggesting that plastic flow is relatively difficult in BASs and the bonding nature in BASs is most probably covalent rather than ionic [35]. As BASs have very high carbon content (15 %) [1-3, 6, 7, 28, 29] which supports this fact as most of the carbon containing materials or compounds are mostly covalent.

Vicker's indents were observed in optical and stereo scan as well as in scanning electron microscopes. Semicircular shear bands formation were observed around the Vicker's indents as shown Figure 3(a, b) at two different zones. It shows some ductility in the material. Unlike to previous studies, semicircular slip bands were observed around the indents in the present

Table 3. Comparison of thermal properties of amorphous steels.

| Alloy | $T_g$ | $T_x$ | $\Delta T_x$ | $T_l$ | $T_g/T_l$ | $\gamma$ | $\delta$ | $\beta$ | Reference |
|---|---|---|---|---|---|---|---|---|---|
| $Fe_{50}Cr_{14}Mo_{14}C_{14}B_6Zr_2$ | 798 | 868 | 70 | 1453 | 0.55 | 0.39 | 1.33 | 2.02 | This study |
| $Fe_{50}Cr_{14}Mo_{14}C_{14}B_6Y_2$ | 840 | 908 | 68 | 1435 | 0.585 | 0.399 | 1.526 | 2.75 | [1] |
| $Fe_{50}Cr_{14}Mo_{14}C_{14}B_6Gd_2$ | 840 | 899 | 59 | 1435 | 0.585 | 0.399 | 1.510 | 2.63 | [1] |
| $Fe_{50}Cr_{14}Mo_{14}C_{14}B_6Dy_2$ | 859 | 929 | 70 | 1415 | 0.607 | 0.409 | 1.671 | 3.38 | [2] |
| $Fe_{50}Cr_{15}Mo_{14}C_{15}B_6$ | 829 | 874 | 45 | 1483 | 0.559 | 0.378 | 1.336 | 1.95 | [28] |
| $F_{65}Mo_{14}C_{15}B_6$ | 789 | 843 | 54 | 1418 | 0.556 | 0.382 | 1.340 | 2.01 | [28] |
| $Fe_{63}Mo_{14}C_{15}B_6Er_2$ | 777 | 819 | 42 | 1423 | 0.546 | 0.372 | 1.268 | 1.75 | [28] |
| $Fe_{65}Mo_{14}C_{15}B_6$ | 789 | 843 | 54 | 1418 | 0.556 | 0.382 | 1.340 | 2.01 | [29] |
| $Fe_{63}Mo_{14}C_{15}B_6Er_2$ | 777 | 819 | 42 | 1423 | 0.546 | 0.372 | 1.268 | 1.74 | [29] |
| $Fe_{63}Mo_{14}C_{15}B_6Dy_2$ | 777 | 817 | 40 | 1418 | 0.548 | 0.372 | 1.275 | 1.76 | [29] |

Table 4. Density and mechanical properties of the $Fe_{50}Cr_{15}Mo_{15}C_{16}B_6Zr_2$ BAS and their comparison with other as cast BASs.

| Alloy | ρ (g/cm$^3$) | Vicker's hardness $H_V$ | H (GPa) | E (GPa) | H/E | Reference |
|---|---|---|---|---|---|---|
| $Fe_{50}Cr_{14}Mo_{14}C_{14}B_6Zr_2$ | 7.170 | 1240 | 14.9 | 248.0 | 0.0600 | Present work |
| $Fe_{50}Cr_{14}Mo_{14}C_{14}B_6Y_2$ | 8.431 | 1219 | 17.2 | 263.0 | 0.0652 | [1, 2] |
| $Fe_{50}Cr_{14}Mo_{14}C_{14}B_6Gd_2$ | 8.521 | 1155 | 15.2 | 244.9 | 0.0621 | [1, 2] |
| $Fe_{50}Cr_{14}Mo_{14}C_{14}B_6Dy_2$ | 8.600 | 1272 | 16.7 | 256.9 | 0.0651 | [1, 2] |

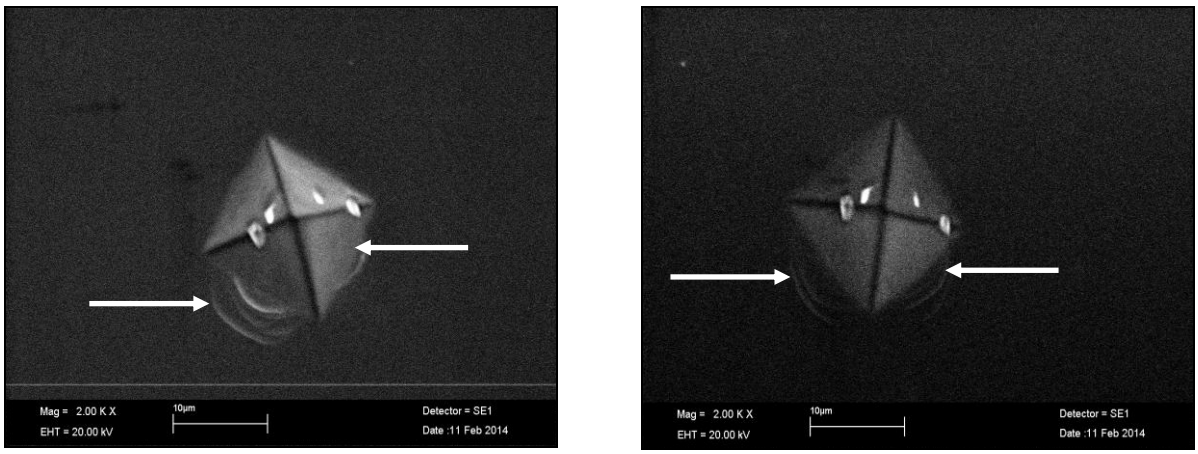


(a) (b)

Figure 3. SEM image of two Vicker's indents at two different areas in amorphous matrix showing semicircular shear bands around the indents indicating plasticity in the material (a, b).

BAS instead of diagonal cracks of Vicker's indents [36]. Semicircular shear bands around Vicker's indent are the clear-cut evidence of a little plasticity in the materials [37].

Compression tests results in the in the fragmentation of the bulk samples into many pieces. In order to study fracture behavior, selected pieces of compression tested specimens were examined in SEM and the results are shown in Figure 4(a-d). Parallel and curved shear bands were mostly observed in the broken samples. It indicates the brittle nature of the BAS studied. It is due to high carbon concentration (14 %) in the alloy. Various zones with different morphologies of shear bands were observed. Different shear planes have different shear angles. In some areas shear bands formation was observed in different directions. Plains having parallel shear bands are blocked by other shear plains having the shear bands at some other angle. The origin of initialization and propagation of shear bands in shear plains is clear in the micrographs. Propagation started from a weak zone containing some defect.

## 4. Conclusions

Bulk ingots of paramagnetic $Fe_{50}Cr_{14}Mo_{14}C_{14}B_6Zr_2$ bulk amorphous steel of 3 mm thickness were produced first time at PINSTECH by arc melter and characterized by XRD, SEM/EDAX and DSC techniques. The results obtained by these techniques are well agreed and confirm the amorphous nature of materials produced. The present BAS have lower density (7.17 g/cm$^3$) than previously reported steels and have better properties. DSC scans shows multistage crystallization. Shear band formation in compression tested fractured samples indicate brittle nature of the BAS. Our findings indicate evidence of covalent bonding in BASs. Melting and liquid temperatures are found to be very high for this BAS. Wide supercooled liquid region of 70 K and γ parameter of about 0.4 indicates good thermal stability and high GFA. The present BAS have very promising thermal properties better than many previously reported BASs. Vicker's microhardness, nanohardness, elastic modulus and fracture strength of $Fe_{50}Cr_{14}Mo_{14}C_{14}B_6Zr_2$ BAS are found to be 1240 $H_V$, 14.9 GPa, 248 GPa and 4.96 GPa respectively indicating promising mechanical properties. Attractive mechanical and thermal properties show that BASs can be used for various industrial applications.

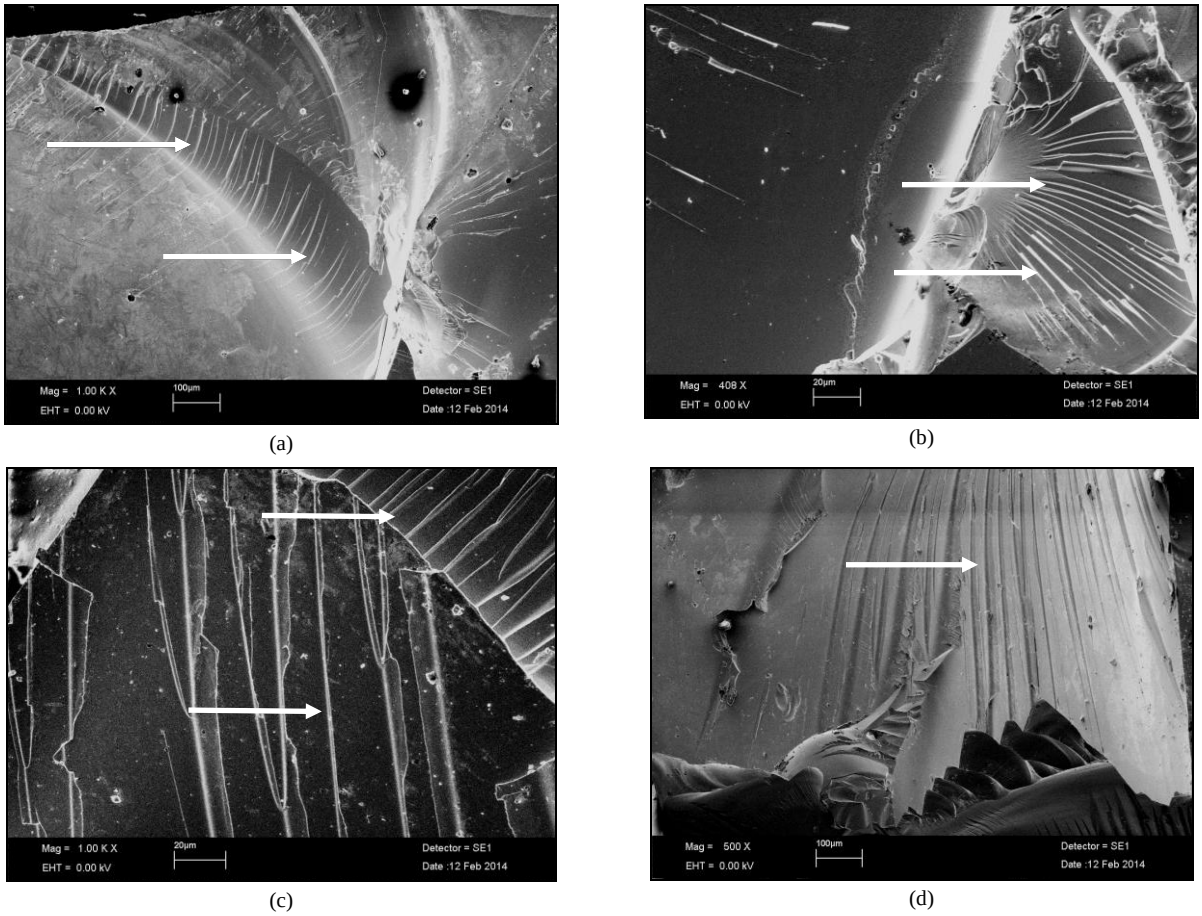


Figure 4 SEM micrographs of the compression tested sample at various magnifications showing parallel and curved shear band formation indicating brittle nature of the BAS (a-d).

## Acknowledgements

The authors gratefully acknowledge the travel grant and the financial support provided by Third World Academy of Sciences (TWAS). The local hospitality provided by the Institute of Physics (IOP), Chinese Academy of Sciences (CAS), Beijing, China is highly appreciated. We are grateful to all members of MSG, PD, PINSTECH, Islamabad, Pakistan and BMG Group, IOP, CAS Beijing, China. Thanks to PAEC for permission to do work at IOP, Beijing, China.

## References

[1] M. Iqbal, J.I. Akhter, H.F. Zhang and Z.Q. Hu, J. Non-Cryst Solids **354** (2008) 3284.

[2] M. Iqbal, J.I. Akhter, H.F. Zhang and Z.Q. Hu, J. Mater. Sci. Technol. **26** (2010) 783.

[3] M. Siddique, M. Iqbal, J.I. Akhter and M. Ahmad, J. Alloy. Compd. **482** (2009) 25.

[4] J.I. Akhter, M. Iqbal, M. Siddique, M. Ahmad, M.A. Haq, M.A. Shaikh and Z.Q. Hu, J. Mater. Sci. Technol. **25** (2009) 48.

[5] M. Iqbal, J.I. Akhter, H.F. Zhang and Z.Q. Hu, J.Non-Cryst. Solids **354** (2008) 5363.

[6] V. Ponnambalam, S.J. Poon and G.J. Shiflet, Appl. Phys. Lett. **83** (2003) 1131.

[7] Z.P. Lu, C.T. Liu, J.R. Thompson and W.D. Porter, Phys. Rev. Lett. **92** (2004) 245503.

[8] Z.P. Lu, C.T. Liu and W.D. Porter, Appl. Phys. Lett. **83** (2003) 2581.

[9] Q.J. Chen, D.L Zhang, J. Shen, H.B. Fan and J.F. Sun, J. Alloy. Compd. **427** (2007) 190.

[10] X.J. Gu, S.J. Poon, G.J. Shiflet and M. Widom, Acta Mater. **56** (2008) 88.

[11] Q.J. Chen, H.B. Fan, J. Shen, J.F. Sun and Z.P. Lu, J. Alloy. Compd. **407** (2006) 125.

[12] S. Ahmadi, H. R. Shahverdi , M. Afsari and A. Abdollah-zadeh, J. Non-Cryst. Solids **365** (2013) 47.

[13] J.W. Li, A.N. He and B.L. Shen, J. Alloy. Compd. **586** (2014) S46.

[14] J.T. Kim, S.H. Hong, C.H. Lee, J.M. Park, T.W. Kim, W.H. Lee, H.I. Yim and K.B. Kim, J. Alloy. Compd. **587** (2014) 415.

[15] Y. Hu, M.X. Pan, L.Liu and W.H. Wang, Mater. Lett. **57** (2003) 2698.

[16] D.R. Maddala and R.J. Hebert, Wear **294** (2012) 246.

[17] J. Schroers, B. Lohwongwatana, W.L. Johnson and A. Peker, Mater. Sci. Eng. A **449-451** (2007) 235.

[18] O.N. Senkov and D.B. Miracle, Mater. Res. Bull. **36** (2001) 2183.

[19] A. Takeuchi and A. Inoue, Mater. Trans. **46** (2005) 2817.

[20] Z. P. Lu, H. Bei and C.T. Liu, Intermetallics **15** (2007) 618.

[21] Q.J. Chen, J. Shen, D. L. Zhang, H.B. Fan, J.F. Sun and D.G. McCartney, Mater. Sci. Eng. A **433** (2006) 155.

[22] Z.Z. Yuan, S.L. Bao, Y. Lu, D. P. Zhang and L. Yao, J. Alloy. Compd. **459** (2008) 251.

[23] Z.L. Long, G. Xie, H. Wei, J. Peng, P. Zhang and A. Inoue, Mater. Sci. Eng. A **509** (2009) 23.

[24] A. Hruby, Czech. J. Phys. B **22** (1972) 1187.

[25] M. Saad and M. Poulain, Mater. Sci. Forum **19** (1987) 11.

[26] Y. Li, J. Mater. Sci. Technol. **15** (1999) 97.

[27] M.L.F. Nascimento, L.A. Souza, E.B. Ferreira and E.D. Zanotto, J. Non-Cryst. Solids **351** (2005) 3296.

[28] X.J. Gu, S. J. Poon and G. J. Shiflet, J. Mater. Res. **22** (2007) 344.

[29] X.J. Gu, A.G. McDermott, S.J. Poon and G.J. Shiflet, Appl. Phys. Lett. **88** (2006) 211905-1.

[30] M. Iqbal, J.I. Akhter, Z.Q. Hu and H.F. Zhang, J. Non-Cryst. Solids **354** (2008) 3291.

[31] M. Iqbal and W.H. Wang, J. Phys: IOP Conference Series: Mater. Sci. Eng. **60** (2014) 012003.

[32] M. Iqbal, J.I. Akhter, M.U. Rajput, K. Mahmood, Z. Hussain , S. Hussain and M. Rafiq, Key Engg. Mater. **510-511** (2012) 137.

[33] M. Iqbal and W.H. Wang, J. Phys: IOP Conference Series: Mater. Sci. Eng. **60** (2014) 012035.

[34] W.H. Wang, J. Appl. Phys. **99** (2006) 093506-1.

[35] J.G. Wang, B.W. Choi, T.G. Nieh and C.T. Liu, J. Mater. Res. **15** (2000) 798.

[36] M. Iqbal, Ph. D Thesis (2008) Chapter 5 pp.145-185, Institute of Metal Research, Chinese Academy of Sciences, Shenyang, P. R. China.

[37] M. Iqbal, J.I. Akhter, M. Ahmad, H. F. Zhang and Z. Q. Hu, 3rd international conference on frontiers of advanced engineering materials (FAEM-08/01) (2008) 1.